Transmission and Thermal Emission in the NO₂ and CO Absorption Lines using Macroporous Silicon Photonic Crystals with 700 Nm Pitch

D. Cardador, D. Segura, D. Vega and A. Rodríguez

Micro i Nanotecnologies, Departament d'Enginyeria Electrònica, Universitat Politècnica de Catalunya,
C/Jordi Girona, 31, 08031, Barcelona, Spain

Keywords: Photonic Crystals, Pitch, Cavity, Resonance, Transmission, Emission, Q-factor, Gas Sensor.

Abstract: Macroporous silicon photonic crystals with a cavity in the middle of their structure have been studied in both, transmission and emission. The initial transmittance of the photonic crystals was increased form 4%-6% up to the value of 25%-30% by performing a rear attach of the samples of approximately 160 µm. The use of wafers with 700 nm of pitch allowed us to fabricate the optical response of the photonic crystals in the ranges of 6.4 µm and 4.6 µm, where different gases have their absorption frequency –such as NO₂ or CO. The fabricated samples have been also heated in order to evaluate their viability to be used as selective emitters for gas sensing purposes. Results show a good agreement in the position of the respective peak compared to the transmission spectrum. However, further studies have to be done to place the base of the peak as close as possible to the 0% of emission in order to have a better selective emitter. This work is a starting point for gas detection devices using macroporous technology in the mid-infrared, which includes ammonia, formaldehyde, carbon monoxide or nitrous oxide, among others.

1 INTRODUCTION

Photonic Crystals (PC) are becoming increasingly attractive for both research and market applications. Their optical properties, obtained by creating periodical structures of different refractive index materials, are very interesting for a wide range of application areas, such as optical communications or sensing. The introduction of defects in the structure that break the periodicity confers the PC some interesting functionalities. They allow the creation of resonant states within the photonic bandgap at specific frequencies or modes -(Joannopoulos et al. 2011; Braun et al. 2006)- what can be used as waveguides (Rinne et al. 2007), light couplers, optical resonators (Youcef Mahmoud et al. 2012), thermal emitters (Gesemann et al. 2010) or tuneable filters (Neumann et al. 2008), etc.

As reported in the literature, there are several factors that affect the photonic bandgap features: the contrast between the high and the low reflective index in the PC, the morphology, the light path, etcetera (Joannopoulos et al. 2011). In the case of introducing a defect inside the photonic crystal, it is also important to have into account its shape to predict the optical response of the structure. Several articles have dealt with this issue in 1D and 2D PCs −i.e. (Alvarado-Rodriguez 2003; Xiao et al. 2016; Mohebbi 2015). However, the influence of the defects morphology in the optical response of 3D photonic crystals have not been so deeply analysed, perhaps, because of the high dependence of the method used to fabricate the PC (Nelson 2011; Braun et al. 2006b). A number of different techniques have been proposed to incorporate defect structures within the PCs in woodpiles (Taverne et al. 2015), synthetic opals (Massé et al. 2006; Palacios-Lidón et al. 2004) or macroporous silicon (Mertens et al. 2005), among others.

In this paper we focus on macroporous silicon (mp-Si), which is a versatile material that can be successfully fabricated through the so-called *electrochemical etching* (EE). With this technique it is possible to fabricate pores with different depth profiles -such as sinusoidal or straight- with a planar defect inside the crystal structure –see Fig. 1. Previous studies reported mp-Si structures with a cavity in the middle of the PC that had a resonant wavelength around the 7 µm (Mertens et al. 2005). Nevertheless, they worked with a lattice parameter –

191

also called pitch- of 2 µm and a vertical periodicity about 2.5 µm. This vertical periodicity is limited to the lattice parameter: when approaching to the pitch value, the vertical periodicity is more difficult to achieve and the profile is much more difficult to control by EE. Although some other studies reported modulated structures in 700 nm (Langner 2008), they did not insert a cavity in their structures, probably because the profiles were not as good as the ones obtained in 2 µm of pitch. In the present study, the samples used to fabricate the macroporous silicon PCs had a pitch of 700 nm and a vertical periodicity around the lattice parameter, what enabled us to place a peak and tailor it at wavelength as short as 4.6 microns, were different gas absorption peaks can be found.

By removing around 160 µm of bulk silicon of the samples, we have been able to increase the transmission percentage from values around 4%-6% up to values between 25% and 30%. This improves the features of the peak –i.e. transmittance and quality factor- and, as a consequence, the sensitivity of the final gas sensor device is enhanced. Further improvement of the transmission could be achieved by removing some more bulk silicon, but the risk of damaging the photonic crystal –mechanical support or etching of the PC structure- becomes high and some silicon bulk has to be left to avoid these problems. In the case of thermal emission this layer has not an important impact in the relative transmission amplitude of the peak –from the base to the top of the resonant peak-, but it has a considerable effect in the position of the base point. Specifically, the more bulk silicon the more radiation of the no texturized region, which is finally reflected in a higher offset from the zero emission point to the base point, where the emission peak rises.

The conclusions drawn in this paper lead us to confirm that the studied macroporous silicon structures can be employed in gas sensing applications. However, further work has to be done in order to improve the amplitude and the Q-factor of the peak, as well as to reduce the offset, either working in transmission or emission.

2 EXPERIMENTAL

The 3D structures were obtained by electrochemical etching of *n*-type (100) crystalline silicon samples in hydrofluoric (HF) acid solution. The starting material had a resistivity between 0.1-0.3 Ω·cm

($\sim3\cdot10^{16}$/cm^3 phosporous-doped). An N^+ layer was implanted on the backside of the wafer to provide a low-resistance transparent ohmic contact. Next, the wafer was oxidized and a nanoimprint lithography of 700 nm pitch was performed. A Reactive-ion Etching (RIE) and a tetramethylammonium hydroxide (TMAH) etching were done to create inverted pyramid-shaped pits that act as nucleation centres for the ordered pore growth. Finally, the EE etching was carried out to control the modulation of pore diameter which, is regulated by the applied etching current. This method allows to design the profile beforehand and to create smooth 3D structures of great complexity just by applying different etching currents.

In particular, the periodical profiles attached in Fig.1 have been generated. In the first sample (left) the depth periodicity was set to be about 1.1-1.2 µm what arouse a bandgap around [5-7] µm. As depicted in the figure, a planar defect was introduced halfway the total pore depth by suppressing one of the modulations and leaving a constant diameter section. The length of the cavity varied from 2.1 µm to 2.6 µm with a diameter of 0.23 µm in all the samples. In order to reduce the bandgap central wavelength, and thus the position of the peak, the vertical modulation of the pore was shortened. In concrete, it was set to the lattice constant value (~700nm). Thanks to that, the bandgap moved to the range of [4-5] µm, while the defect's length took values in the range of [1.5-1.8] µm. The total depth of all samples was about 12-15 micrometers. A complete description of the process can be found elsewhere (Lehmann 1993). The second fabricated structure can be observed in the right image.
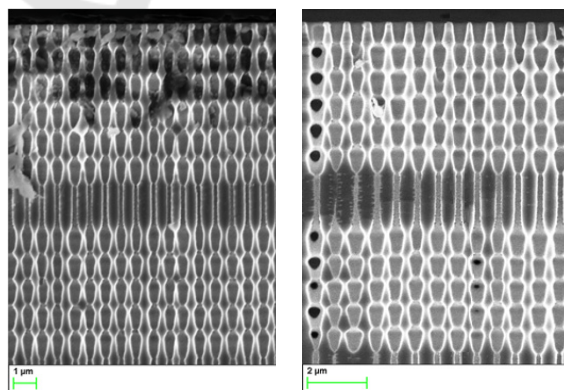

Figure 1: Cross sectional view of two 3-D PCs fabricated by EE over a litography of 0.7 µm pitch. The inclusion of a defect in the PC lattice enables a transmitted mode in 6.4 µm (left) and 4.6 µm (right). (les he reordenat en l'ordre del text).

The transmitted response of the fabricated samples was measured in the MIR range using a Bruker Optic's Vertex FT-IR spectrometer. The lattice was aligned to the $\Gamma - M$ direction (along one lattice axis in the surface), an aperture of 1 mm and a resolution of 4 cm^{-1} was used for the calculation of the spectrum. The measurements have been referred to the source spectrum to normalize the results.

The emissivity was experimentally measured using the A540 emission adapter of the FT-IR spectrometer. This commercial setup allows normal thermal emission measurement, with a beam opening angle of ±7,5°, from room temperature up to 400 °C. In this setup, the sample is clamped vertically to a metallic surface that is at a constant temperature. After thermalization, the sample is at a constant and homogeneous temperature very close to the temperature of the heater, since c-Si is an excellent thermal conductor. In our case, the samples were heated at the highest possible temperature in order to obtain the maximum power of the emitter. Finally, the emissivity values are obtained after conducting a standard calibration with a piece of polished Si as reference.

3 RESULTS AND DISCUSSIONS

The two fabricated samples of the Figure 1: are characterized in the FT-IR. In the Figure 2: the sample's transmission spectrum is shown. As depicted in it, there is a high enhancement in the transmission due to the reduction of, approximately, 160 μm of bulk silicon from the back side of the wafer. In particular, the transmission percentage rises from the value of 6% up to 29%. Previous studies reported maximal transmission peaks of almost 50% using mp-Si structures. Nonetheless, their peaks were placed out of the mid-infrared range –following the same convention as in (Byrnes 2008)- in concrete at 20 μm, far from the interesting gas sensing mid infrared frequencies.
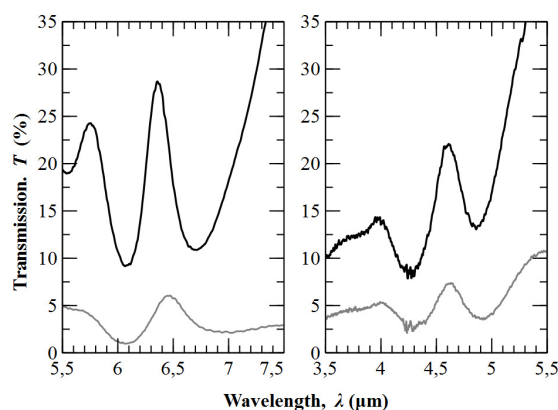

Figure 2: Transmittance of the samples before (grey) and after (black) the TMAH attack for removing part of the bulk silicon of the wafer. The different wavelength range are achieved by controlling the vertically periodicity. Left image corresponds to the image plotted in Fig.1(a) and the right image to the Fig.1(b).

The values presented in this work are the best ones reported in the mid-infrared, as far as our research reached, in 3D mp-Si structures. Moreover, the use of samples with 700 nm of pitch made possible to reduce the vertical modulation and adjust its periodicity close to the lattice constant. This entailed a proportional translation of the entire spectrum towards lower frequencies. An appropriated dimensioning of the defect's length and width lead us to correctly place a resonant mode inside the bandgap. Consequently, we were able to reproduce the transmittance figure around 4.6 μm, where the CO has its absorption lines –see Fig. 2.

As explained in the introduction, below the PC there is some remaining bulk silicon. This silicon reduces the amount of ideally transmitted light, which in simulations –without any bulk silicon- can be around 60%. However the reduction of more silicon presents some problems. The first of them is the risk of damaging the PC structure after some hours of TMAH attack. The second one is that if the attacked surface is big, some mechanical stress can appear, completely breaking the surface as a consequence.

One interesting fact is that by removing some bulk silicon the quality factor of the peak is also enhanced, improving the performance of a future gas sensor. Nevertheless, the transmission inside the band gap is also increased what, in turn, will result in less sensitivity in a gas sensor. Some research should be carried out to reduce the transmission inside the band gap for obtaining good gas sensors.
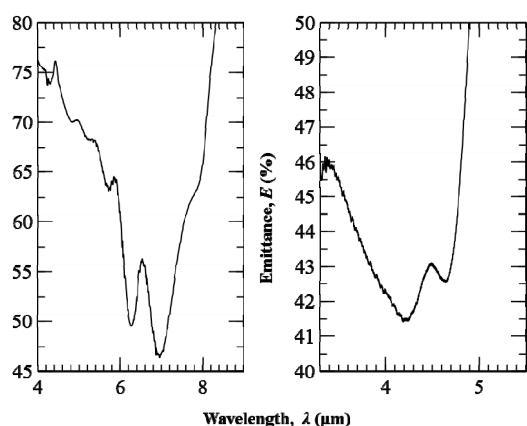
Figure 3: Experimental emisison spectra for the samples depicted in Fig. 1 (they are conveniently depicted. E.g.: left image in Fig. 1 corresponds to the left image in Fig.3). Both samples were heated at 400 ºC.

In the right image of the Fig. 2, it can be seen the trademark of the CO_2 absorption lines at a 4.25 μm wavelength. These marks correspond to variations of gas concentrations referred to the background case. If the peak is positioned on the absorption lines of a target gas, the concentration of it can be determined by comparing the area of the peak before and after the gas exposure. Even more, despite using the PC for filtering the light coming from the emitter, the sample can be heated in order to have an emission peak at the desired wavelengths. This would allow replacing the optical emitter for a selective thermal emitter, emitting in a smaller range of wavelengths, and thus, simplifying the configuration for sensing gases, probably without the need of an optical filter.

The lowered samples were used to evaluate their thermal emission in the two studied wavelengths – see Fig. 3- when the samples are heated at 400ºC. The peaks are placed around 6.5 μm and 4.5 μm, in good accordance with the position of the peak in transmission. If observed insightfully a peak broadening of about 100 nm can be seen in both cases. A reduction of their respective amplitudes, compared to their transmission spectrum, is also noticeable, particularly at 4.5 μm. During the study we have verified that there are some variations in the pore's morphology due to the expansion of the silicon with the heating of the sample, which affects the optical response of the peak; these experimental variations, although they are of a few tens of nanometers, modify the local refractive index what, finally, impacts in the position and the amplitude of the peak.

Another remarkable point is that the peaks do not start at zero position; they have their beginning at the emissivity of 40%-45%. Probably part of this offset is due to the remaining bulk silicon in the bottom of the photonic crystal, which also radiates in the frequencies of the peak, reducing the performance of the samples as selective thermal emitters.

Further studies should deal with this issue in order to obtain good selective emitters that propagate a range of frequencies along its bandgap.

4 CONCLUSIONS

Macroporous silicon photonic crystals with a defect inserted in the middle of the structure have been studied. The initial transmittance of these structures is between the 4% and the 6%. Performing a rear attach of the sample –approximately 160 μm-, the transmission percentage increases to the value of 25%-30%.

The use of samples with 700 nm of pitch allows to work with sub micrometre vertical periods. Thanks to this, peaks at lower resonant frequencies can be placed, in concrete, we have fabricated two of them: at 6.4 μm and 4.6 μm, what can be used to sense different gases that have their absorption frequency in ranges close to that values –such as NO_2 or CO.

Both peaks been heated at room temperature of 400 ºC in order to obtain a selective emitter. Results show a good agreement in the position of the peak compared to the position in the transmission spectrum. The little differences are attributable to the variations in the shape of the pores given by the expansion of the silicon due to higher temperatures. Further studies have to be done to place the base of the peak as close as possible to the 0% of emission in order to have a real selective emitter.

This work is a starting point for gas detection devices using macroporous technology in the mid-infrared, which includes ammonia, formaldehyde, carbon monoxide or nitrous oxide, among others.

ACKNOWLEDGEMENTS

REFERENCES

Alvarado-Rodriguez, I., 2003. Fabrication of two-dimensional photonic crystal single-defect cavities and their characterization by elastic scattering. *A*

dissertation Doctor of philosophy in Electrical Engineering.-Los Angeles, University of california.

Braun, P.V., Rinne, S.A. & García-Santamaría, F., 2006. Introducing Defects in 3D Photonic Crystals: State of the Art. *Advanced Materials*, 18(20), pp.2665–2678.

Byrnes, J., 2008. Unexploded ordnance detection and mitigation. Springer Science & Business Media.

Gesemann, B., Schweizer, S.L. & Wehrspohn, R.B., 2010. Thermal emission properties of 2D and 3D silicon photonic crystals. *Photonics and Nanostructures - Fundamentals and Applications*, 8(2), pp.107–111.

Joannopoulos, J.D. et al., 2011. Photonic Crystals: Molding the Flow of Light, Princeton university press (Second Edition).

Langner, A., 2008. Fabrication and characterization of macroporous silicon. *Doktorarbeit, Martin-Luther-Universität*.

Lehmann, V., 1993. The Physics of Macropore Formation in Low Doped n-Type Silicon. *Journal of The Electrochemical Society*, 140(10), p.2836.

Massé, P. et al., 2006. Tailoring planar defect in three-dimensional colloidal crystals. *Chemical Physics Letters*, 422(1-3), pp.251–255.

Mertens, G. et al., 2005. Tunable defect mode in a three-dimensional photonic crystal. *Applied Physics Letters*, 87(24), p.241108.

Mohebbi, M., 2015. Refractive index sensing of gases based on a one-dimensional photonic crystal nanocavity. *Journal of Sensors and Sensor Systems*.

Nelson, E., 2011. Three-dimensional photonic crystal optoelectronics. Diss. University of Illinois at Urbana-Champaign.

Neumann, N. et al., 2008. Tunable infrared detector with integrated micromachined Fabry-Perot filter. *Journal of Micro/Nanolithography, MEMS and MOEMS*, 7(2), p.021004.

Palacios-Lidón, E. et al., 2004. Engineered Planar Defects Embedded in Opals. *Advanced Materials*, 16(4), pp.341–345.

Rinne, S.A., García-Santamaría, F. & Braun, P. V., 2007. Embedded cavities and waveguides in three-dimensional silicon photonic crystals. *Nature Photonics*, 2(1), pp.52–56.

Taverne, M., Ho, Y. & Rarity, J., 2015. Investigation of defect cavities formed in three-dimensional woodpile photonic crystals. *JOSA B*.

Xiao, X. et al., 2016. Investigation of defect modes with Al2O3 and TiO2 in one-dimensional photonic crystals. *Optik - International Journal for Light and Electron Optics*, 127(1), pp.135–138.

Youcef Mahmoud, M. et al., 2012. Optical channel drop filters based on photonic crystal ring resonators. *Optics Communications*, 285(3), pp.368–372.